Opportunities and challenges of transfer reactions at HIRFL-CSRe*

W. W. Wan (万文武)[1] S. Q. Liang (梁诗琪)[1] J. L. Lou (楼建玲)[1†] D. Y. Pang (庞丹阳)[2] X. L. Tu (涂小林)[3]
Y. H. Zhang (张玉虎)[3] G. de Angelis[4] G. Kaminski[5] Q. T. Li (李奇特)[1] H. Y. Ge (葛浩煜)[1]
H. Y. Zhu (朱宏渝)[1] B. L. Xia (夏博龙)[1]

[1]School of Physics and State Key Laboratory of Nuclear Physics and Technology, Peking University, Beijing 100871, China
[2]School of Physics, Beijing Key Laboratory of Advanced Nuclear Materials and Physics, Beihang University, Beijing 100191, China
[3]Institute of Modern Physics, Chinese Academy of Sciences, Lanzhou 730000, China
[4]Istituto Nazionale di Fisica Nucleare, Laboratori Nazionali di Legnaro, viale dell'Università 2 I-35020, Legnaro, Italy
[5]Flerov Laboratory of Nuclear Reactions, JINR, Dubna 141980, Russia

Abstract: The opportunities and challenges of performing transfer reactions in inverse kinematics using the ^{16,18}O beams at the experimental Cooler Storage Ring (CSRe) of the Heavy Ion Research Facility in Lanzhou (HIRFL) with the internal gas-jet target are discussed herein. The kinematics, differential cross sections for various transfer reactions using the ^{16,18}O beam with incident energies of 30 and 100 MeV/nucleon, and the H_2- or D_2-gas-jet targets are compared. The ^{16}O beam at 100 MeV/nucleon with an intensity of $\geq 10^6$ pps interacting with the H_2-gas-jet target is recommended as the first transfer reaction at HIRFL-CSRe.

Keywords: transfer reaction, internal gas target, kinematics, differential cross sections

DOI: 10.1088/1674-1137/add099 **CSTR:** 32044.14.ChinesePhysicsC.49074006

I. INTRODUCTION

Single-nucleon transfer reactions serve as effective probes for studying single-particle structures of nuclei, providing access to extracting spectroscopic factors (SFs), spin-parity (J^π), and effective single-particle energies (ESPEs) [1–5]. Additionally, cluster transfer reactions, such as (p, t), (p, ^{3}He), (d, ^{4}He), and (d, ^{6}Li), are useful for investigating the nucleon-nucleon correlation and 2n-, d-, and α-cluster structures [6, 7]. We have completed several transfer reaction experiments in inverse kinematics [8–19] using radioactive beams (20–30 MeV/nucleon) impinging on solid CH_2 and CD_2 targets at the Radioactive Ion Beam Line in Lanzhou (RIBLL) [20] and Exotic Nuclei Beam Line (En-course) at the Research Center for Nuclear Physics (RCNP), Osaka University [21, 22]. The evolution of intruder s- and d-wave intensities in the N = 8 isotones, referring to ^{12}Be, ^{13}B, and ^{14}C, were deduced from the single-neutron transfer reactions [10, 11, 14]. Resonances in ^{12}Be and ^{13}B were first observed using the missing mass (MM) method [13, 15], which is a key technique for studying unbound states.

An internal gas-jet target [23] has been established at the experimental Cooler Storage Ring (CSRe) [24] of the Heavy Ion Research Facility in Lanzhou (HIRFL) [25], enabling direct nuclear reaction experiments at CSRe. The maximum thickness achieved for the H_2-gas-jet target is 6.6×10^{12} atoms/cm^2, with a background pressure of 10^{-11} mbar in CSRe. The target thickness is adjustable by controlling the nozzle temperature and inlet gas pressure. Using the H_2-gas-jet target, Tu *et al*. studied the elastic scattering of medium-heavy nuclei on protons [26–30]. However, transfer reactions have not been performed at HIRFL-CSRe.

This paper examines the opportunities and challenges of conducting transfer reactions at HIRFL-CSRe, focusing on kinematics, differential cross sections (DCSs), and Q-value resolution for various transfer reactions. The primary beams of ^{16}O and ^{18}O at incident energies of 30 and 100 MeV/nucleon are selected owing to their widespread usage and high-intensity production capabilities. Thus, they are appropriate for the first transfer reaction at HIRFL-CSRe. Additionally, the SFs of ^{16,18}O(p, d), (p, t), (p, ^{3}He) can be extracted by normalizing the experimental differential cross sections to the distorted wave Born approximation (DWBA) calculations. The SFs provide crucial information for investigating the single-neutron strengths in the $^{16,18}O_{g.s.}$ and the quenching effect in transfer reactions [31], which are fundamentally connected to

Received 2 March 2025; Accepted 24 April 2025; Published online 25 April 2025

* Supported by the National Key Research and Development Program of China (2023YFA1606702), the National Natural Science Foundation of China (12275007), and the funding from Heavy Ion Research Facility in Lanzhou (HIR2021PY002)

† E-mail: jllou@pku.edu.cn

the nucleon-nucleon correlations [32]. Furthermore, the relative *nn*-pairing and *np*-pairing strengths in $^{16,18}O_{g.s.}$ can be probed via the SF ratio between the (p, t) and (p, ^{3}He) reactions, which may provide insights into the unexpected findings in ^{12}C, referred to as the relative probabilities of *pp* and *nn* versus *pn* in ^{12}C [33].

II. EXPERIMENTAL SETUP AND KINEMATICS

Figure 1 shows the detailed structure of the internal gas-jet target at HIRFL-CSRe [23]. To measure transfer reactions, a telescope comprising a 300-μm double-sided silicon strip detector (DSSD) and two 1500-μm large surface silicon detectors (SSDs) is recommended at CF100, which is centered at 35° relative to the beam line. Both the DSSD and SSDs share identical dimensions of 64 mm × 64 mm. This telescope has been effectively utilized in the elastic scattering measurement [26–29]. The angular coverage is 14.5°–55.6°, 19.2°–50.8°, and 22.3°–27.7° when the telescope is placed 12, 16, and 20 cm from the center of the gas-jet target, respectively. The corresponding solid angles are estimated to be 0.28, 0.16, and 0.14 sr, assuming the beam is a point source. To measure the recoil light particles from transfer reaction after comprising the angular resolution and the coverage (acceptance), we adopt a distance of 12 cm between the target and DSSD centers in the following text.

In principle, the D_2-gas-jet target can be easily employed in future experiments. Thus, transfer reactions using the D_2-gas-jet target are also discussed in this paper. For the H_2- and D_2-gas-jet targets, the telescope centered at approximately 35° can measure the target-like particles from potential transfer reactions of (p,d), (p,t), (p,^{3}He), (d,t), (d,^{3}He), and (d,^{4}He) with the ^{16,18}O beam in inverse kinematics. The corresponding kinematics of recoil target-like particles from these reactions are shown in Fig. 2 and Fig. 3. The shadows in Fig. 2 and Fig. 3 represent the detection ranges when the telescope is placed 12 cm from the gas-jet target center. This detector cannot measure charged particles with energies above 100 MeV/nucleon, as their energy deposition falls below its detection threshold of 0.4 MeV [29]. Kinematics at a higher beam energy of 100 MeV/nucleon (solid curves), currently achievable at CSRe, are compared with those at a lower energy of 30 MeV/nucleon (dashed curves), which is planned for future implementation. Although lower-energy beams are easily produced at RIBLL and En-course, these facilities lack pure H_2/D_2 gas targets and 10^6 Hz beam revolution frequency. We found that only part of the transfer reaction events will be measured (shadows), which can be clearly seen in both Fig. 2 and Fig. 3. In most cases, only the low-energy branch of recoil particles can be measured with sufficient statistics (typically with a statistical error ≤ 10%) within a limited beam time after considering the DCSs. Nearly all the low-energy branch events (except the events at angles less than 14°) are in the detection ranges whether the incident energy is 100 or 30 MeV/nucleon.

For the H_2-jet-gas target, as shown in Fig. 2, the beam energy of 100 MeV/nucleon (solid curves) provides a larger detection range compared with 30 MeV/nucleon (dashed curves) for most reaction channels, particularly for all ^{16}O-induced reactions and the ^{18}O(p,^{3}He)^{16}N reaction. However, the beam energy has a negligible influence on the detection range for the D_2-jet-gas target (see solid curves comparing with the corresponding dashed curves in Fig. 3). It may be attributed to the very negative Q-values of ^{16}O(p, t)^{14}O (Q = –20.41 MeV), ^{16}O(p,

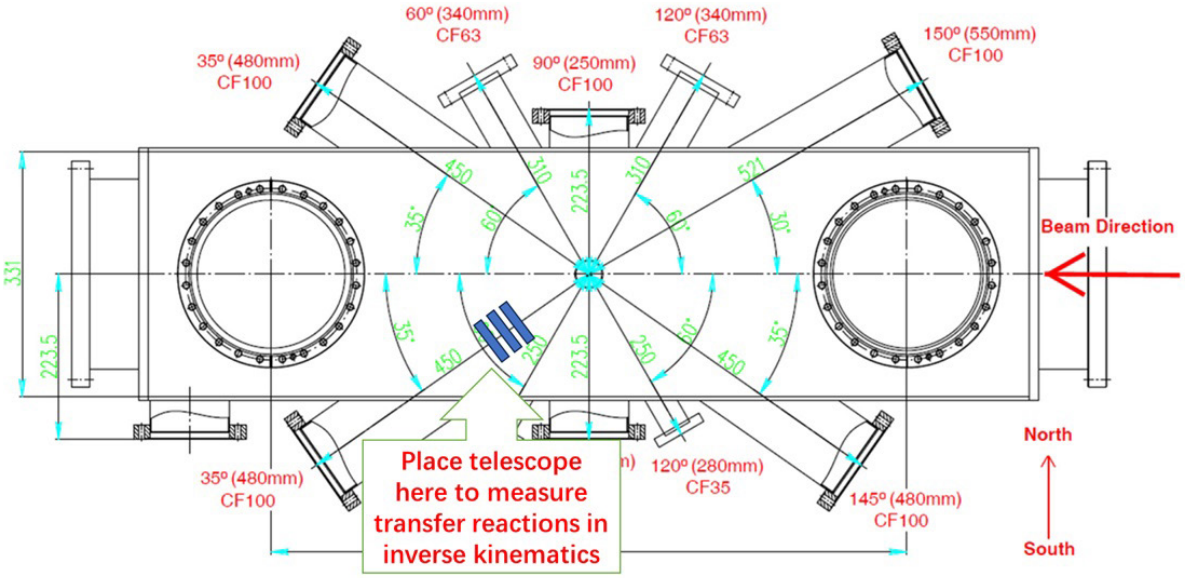

Fig. 1. (color online) Schematic of the internal gas-jet target at HIRFL-CSRe [23]. To measure transfer reactions, a telescope comprised of one DSSD and two SSDs (three blue frames) is installed at CF100 with a centering angle of 35°.

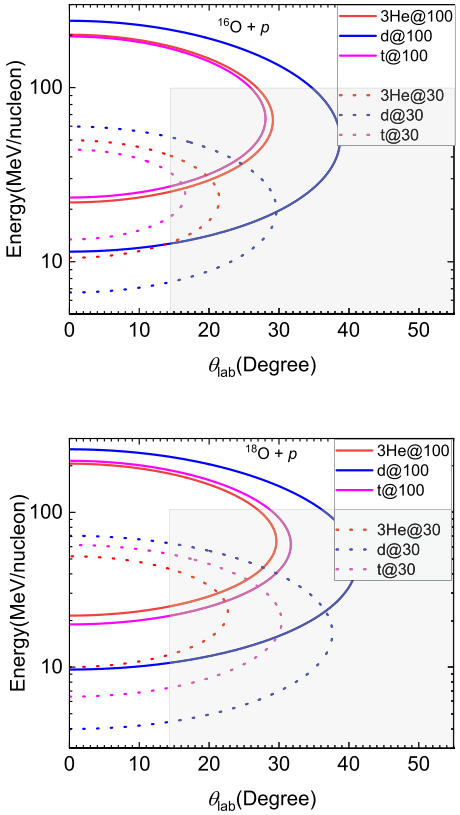

Fig. 2. (color online) Kinematics of the target-like particles emitting from the transfer reactions of ^{16}O + p and ^{18}O + p. Shadows represent the detection range of the telescope. The solid and dashed curves represent the kinematics with beams at incident energies of 100 and 30 MeV/nucleon, respectively.

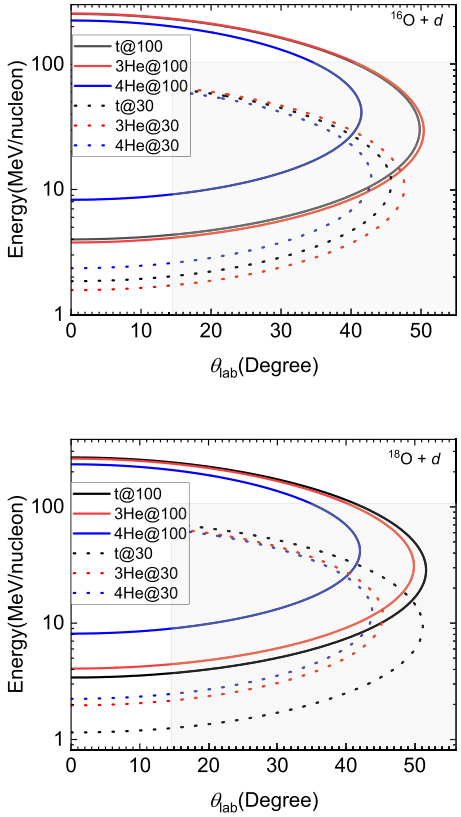

Fig. 3. (color online) Same as Fig. 2 but for the deuteron target.

^{3}He)^{14}N (Q = –15.24 MeV), ^{16}O (p, d)^{15}O (Q = –13.44 MeV), and ^{18}O(p, ^{3}He)^{16}N (Q = –14.11 MeV) compared to ^{18}O(p, t)^{16}O (Q = –3.71 MeV) and ^{18}O(p, d)^{17}O (Q = –5.82 MeV), as well as the relatively lower center-of-mass energy with the proton target in comparison to the deuteron target.

III. DIFFERENTIAL CROSS SECTIONS

Various transfer reaction DCSs of ^{16,18}O on protons and deuterons were calculated in the framework of DWBA with the code of TWOFNR [34]. The global optical potential parameters deduced from the elastic scattering DCSs of many stable nuclei on protons, deuterons, and A = 3 nuclei including tritons and ^{3}He were adopted for the calculations. CH89 [35] and Daehnick [36] were adopted for the entrance channels of transfer reactions on the proton and deuteron targets, respectively. Daehnick [36] was also employed for the exit channel of (p, d), whereas GDP08 [37] was applied for the exit channels of (p, t), (p, ^{3}He), and (d, ^{3}He).

Only the ground states of the residual nuclei were considered in the calculations of DCSs. For example, only the DCSs of ^{16}O(p,^{3}He) to the ground state of ^{14}N (J^{π} = 1^{+}) were calculated. For the single-neutron transfer reactions, referred to as (p, d) and (d, t), the neutron with angular momentum of l = 1 and l = 2 was transferred from ^{16}O and ^{18}O to produce ^{15}O (J^{π} = 1/2^{-}) and ^{17}O (J^{π} = 5/2^{+}), respectively. The single proton with the same angular momentum of l = 1 was transferred from ^{16}O and ^{18}O to populate the ground states of ^{15}N (J^{π} = 1/2^{-}) and ^{17}N (J^{π} = 1/2^{-}), respectively. For the two-nucleon transfer reactions, both the 2n in the (p, t) reaction and the np in the (p,^{3}He) reaction were assumed to be a cluster and only the one-step transfer was considered in calculations. The binding potentials of 1n, 1p, as well as 2n- and np-cluster in ^{16,18}O were assumed to be a Woods-Saxon potential. The geometric parameters of a = 0.65 fm and r = 1.25 fm were fixed, whereas the depth of Woods-Saxon potential was adjusted automatically to reproduce the experimental data of binding energies.

The calculation results for various transfer reactions of ^{16,18}O + p and ^{16,18}O + d are depicted in Fig. 4 and Fig. 5, respectively. Note that the DCSs in the laboratory frame for the low-energy branch of recoil target-like particles are depicted. The shaded regions in Fig. 4 and Fig. 5 represent the accepted angular coverage of the telescope. The laboratory-frame angles are used for following reasons. First, it simplifies the visualization of the de-

tection range for different reaction channels. Second, the statistics of various reaction channels under identical beam time, target, and solid angles are easy to compare. Third, the maximum angle of each channel (in Fig. 4 and Fig. 5), which is kinematically constrained, is clearly visible.

For the H_2-gas-jet target (Fig. 4), the DCSs at 100 MeV/nucleon (dashed curves) for both the ^{16}O and ^{18}O beams are clearly smaller than the corresponding ones at 30 MeV/nucleon (solid curves). However, the maximum angles of target-like particles increase significantly from 30 to 100 MeV/nucleon, resulting in a larger angular coverage for transfer reactions. Despite the incident energy being 100 MeV/nucleon, the DCSs at most accepted angles exceed 1 mb/sr, which is required based on the statistical estimations within a limited beam time. For both ^{16}O and ^{18}O, the DCSs of two-nucleon transfer reactions (thick curves), including (p, ^{3}He) and (p, t), are larger than single-nucleon transfer reactions (thin curves) at the same angles. This indicates that protons, deuterons, tritons, and He isotopes will be measured by the telescope simultaneously. Therefore, particle identification (PID) is important for discriminating different reaction channels. We also found that the DCSs of identical reaction channels, such as (p, ^{3}He) (red curves), with the ^{16}O beam are significantly different from those with the ^{18}O beam, which may be due to the transferred cluster occupying different orbitals and having different node numbers.

For the D_2-gas-jet target, only the DCSs of single-nucleon transfer reactions (d, t) and (d, ^{3}He) are plotted in Fig. 5. The DCS shapes for ^{16}O(d, t) and ^{16}O(d, ^{3}He) are nearly identical owing to the similar quantum numbers and binding energies of the transferred neutron and proton in ^{16}O. In contrast, the DCS shapes for ^{18}O(d, t) and ^{18}O(d, ^{3}He) differ significantly, demonstrating the resolution power of different angular momentums of transfer reactions. Note that the solid and dashed curves in Fig. 5(b) represent the incident energies of 30 and 100 MeV/nucleon, respectively. The angular momentum resolution power at these higher beam energies appears to be comparable to the traditional low-energy measurements for this proposed experiment. Comparing Fig. 5 to Fig. 4, we found that the DCSs are several magnitude lower than those with the H_2-gas-jet target. Thus, the deuteron target is not recommended for initial transfer reaction experiments at HIRFL-CSRe. If we intend to use it in the future, the incident energy of 30 MeV/nucleon is more preferable than 100 MeV/nucleon, as shown in Fig. 5, because the DCSs at most angles exceed 1 mb/sr, which is

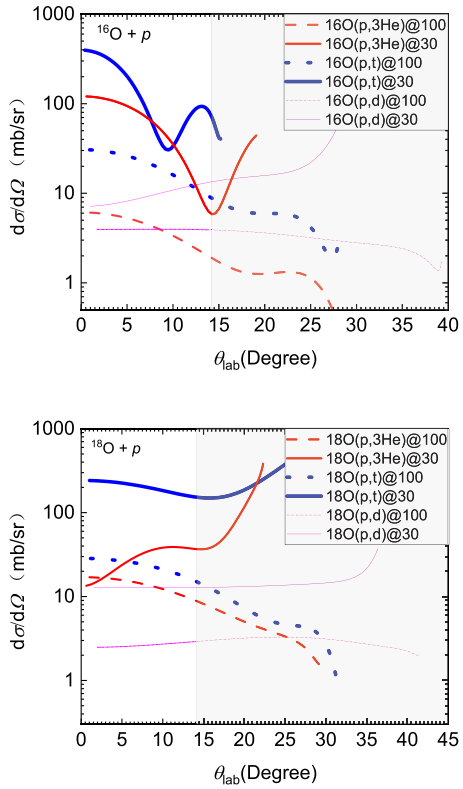

Fig. 4. (color online) Calculated differential cross sections in the laboratory frame for the low-energy branch of the target-like particles recoiling from various transfer reactions. Solid and dashed curves respectively represent two incident energies 30 and 100 MeV/nucleon for both ^{16}O and ^{18}O.

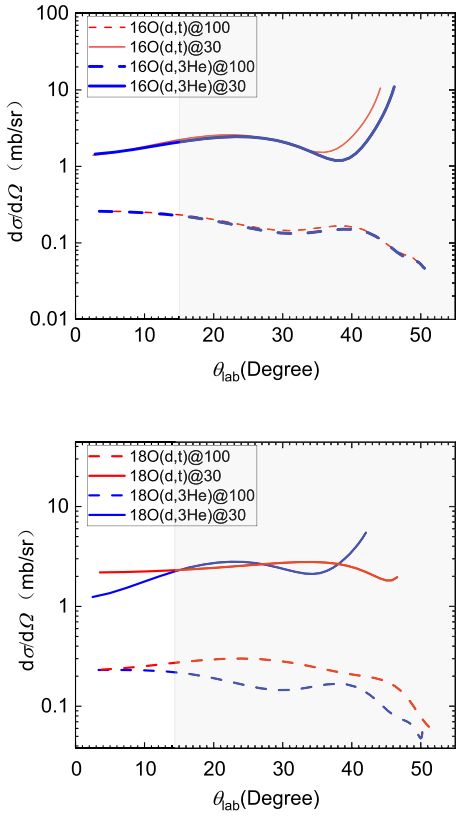

Fig. 5. (color online) Same as Fig. 4 but for the deuteron target.

required by the statistics in a limited beam time.

IV. DISCUSSION

A. Advantages and Feasibility

The primary advantages of performing transfer reaction at HIRFL-CSRe are a good resolution of Q-value spectrum and 10^6 Hz revolution frequency of the stored beam ions. According to previous experimental results, the target thickness, beam energy spread, and energy and angular resolution of detectors contribute the resolution of Q-value spectrum reconstructed using the MM method. The thickness of the internal H_2-gas-jet target (6.6×10^{12} atom/cm^2) is equivalent to the 5.1×10^{-8}-mg/cm^2 solid CH_2 target. This thickness is eight orders of magnitude lower than the typical CH_2 targets (several mg/cm^2) used in our previous experiments, reducing energy losses of recoil target-like particles to the milli-electronvolt level and making their contribution to Q-value resolution negligible. Additionally, the angular dispersion and energy loss of the stored beam ions can be compensated by the electron cooler, enabling the ions to continue circulating in the ring for multi-pass experiments. Therefore, the contribution from the beam ions to the Q-value spectrum can also be ignored. Finally, the detector properties, including energy and angular resolution, are the primary contributors. The simulated Q-value resolutions are listed in Table 1, which are worse than that from elastic scattering [29]. This difference may result from the lower angular resolution of the DSSD and the higher energy of both beam and recoil light charged particles. For instance, a reduction in the incident energy from 100 to 20(30) MeV/nucleon leads to a corresponding decrease in the energy of the recoil charged particle, thereby significantly improving the Q-value resolution for the ^{16}O(p, d)^{15}O reaction from 0.67 to 0.14(0.29) MeV. However, these resolutions are sufficient to discriminate the ground states from the first excited states of residual nuclei ^{15}O, ^{14}O and ^{14}N. Moreover, the 10^6 Hz revolution frequency of the stored ions enhances the beam intensity by a factor 10^6.

Table 2 compares the ^{16}O(p, d)^{15}O experiment planned to be performed at HIRFL-CSRe with our previous ^{13}B(p, d)^{12}B experiment [14]. Several data points are required to determine the angular distributions; therefore, we intend to integrate the events within 4° as a data point. Under the assumptions of a solid angle of 0.02 sr (4° interval), an average DCS of 1 mb/sr, and a beam intensity of 10^6 pps, one ^{16}O(p, d)^{15}O event per hour is expected for each data point. Therefore, a 100 h beam time is required to accumulate 100 events with a statistic error of 10% for each data point. More events can be measured for the ^{16}O(p, t)^{14}O and ^{16}O(p, ^{3}He)^{14}N reactions owing to the larger DCSs, as shown in Fig. 4. These calculations demonstrate the feasibility of transfer reactions using the ^{16}O beam and the ultra-thin internal gas-jet target at HIRFL-CSRe.

Table 1. Simulated resolutions of Q-value spectra reconstructed from the MM method. We assumed that the telescope is placed 12 cm away from the target center, the energy resolution of silicon detector is 1%, and angular resolution of the telescope is deduced from the strip width of 2 mm. The incident energy of ^{16}O is 100 MeV/nucleon.

Reaction channels	σ/MeV
^{16}O(p, d)^{15}O 100 MeV/nucleon	0.67
^{16}O(p, t)^{14}O 100 MeV/nucleon	1.05
^{16}O(p, ^{3}He)^{14}N 100 MeV/nucleon	1.04
Elastic scattering[29]	$\leq$ 0.50

Table 2. Comparison of the ^{16}O(p, d)^{15}O experiment planed to be performed at HIRFL-CSRe with our previous ^{13}B(p, d)^{12}B experiment [14].

	^{16}O(p, d)^{15}O	^{13}B(p, d)^{12}B [14]
beam energy(MeV/nucleon)	100	23
beam intensity (pps)	$\geq 10^6 \times 10^6$	2×10^4
target thickness (atomic/cm^2)	6.6×10^{12}	8.71×10^{20}
average DCS (mb/sr)	1.0	1.0
statistic of each point(counts/h)	1.0	2.5

B. Challenges

Compared with our previous experiment, several new challenges must be considered before conducting the experiment. First, the installation of the telescope closer to the beam line to enhance the angular coverage, such as 12 cm from the gas-jet center. Second, determining the emitting angles of target-like particles in the absence of tracking information (no position information of beam ions impinging on the gas-jet target), which will largely affect the Q-value resolution and solid angles. Third, the CsI(Tl) detector, commonly used to measure the residual energy, cannot be employed at HIRFL-CSRe to maintain the ultra-high vacuum of the storage ring. Thus, higher-energy target-like particles will punch through the silicon detector, complicating the total energy measurement without unambiguous PID. Finally, the counting of the beam ions without the beam monitor as well as the measurement of the thickness of the gas-jet target. These two values are important for extracting the experimental DCSs of transfer reactions.

To solve these challenges, we must improve the telescope and its frame described in Sec. II. We suggest adding a 1500-μm DSSD behind the 300-μm DSSD. Two DSSDs in a telescope can track target-like particles to determine their emitting angles. For particles penetrating

the telescope, the ΔE-ΔE method will distinguish $Z = 1$ particles from $Z = 2$ particles. Subsequently, with different particle assumptions, we deduce the total energy using the energy losses in the silicon detector and its actual thickness. Finally, particle type will be determined using the χ^2 minimum method, comparing total energy versus angle with the kinematics in Fig. 2 and Fig. 3. Additionally, we must develop the stopping detectors that can function in the ultra-high vacuum of CSRe. A Schottky pickup is typically employed in storage rings to monitor beam ions. However, determining the luminosity for in-ring reaction measurements remains challenging, owing not only to temporal variations in beam intensity and gas-target density but also to uncertainties in the beam–target overlap [38]. A dual-measurement approach is often adopted to address this, wherein experimental cross sections are normalized to well-established reference cross sections. In our case, the product of beam ions × target thickness can be calibrated using either simultaneously measured elastic scattering data [30] or the spectroscopic factor derived from the single-neutron transfer reaction of ^{16}O via the summing rule [1].

V. SUMMARY

We evaluated the feasibility, advantages, and challenges of measuring transfer reactions using the ^{16,18}O beams and the existing internal gas-jet target at HIRFL-CSRe. Key considerations included the target structure, reaction kinematics, differential cross sections, Q-value resolution, and statistical requirements. Based on the above discussion, incident energies of 100 MeV/nucleon for the H_2 target and 30 MeV/nucleon for the D_2 target were recommended to optimize transfer reaction measurements within a limited beam time. Considering current experimental conditions, the ^{16}O beam at 100 MeV/nucleon with an intensity larger than 10^6 pps impinging on the H_2-gas-jet target can be considered as the first attempt of transfer reactions.

References

[1] W. Liu, J.L. Lou, Y.L. Ye *et al.*, Nucl. Sci. Tech. **31**, 20 (2020)
[2] S. L. Chen, Z. X. Liu, Zh. Zhang *et al.*, Chin. Phy. C. **48**(7), 074104 (2024)
[3] Y. P. Xu, S. L. Chen, D. Y. Pang, Nucl. Sci. Tech. **35**, 13 (2024)
[4] W. J. Kong and D. Y. Pang, Nucl. Sci. Tech. **34**, 95 (2023)
[5] G. Li, Z. W. Tan, J. L. Lou *et al.*, Nucl. Phys. Rev. **37**(3), 426 (2020)(in Chinese)
[6] A. Lemasson, A. Navin, M. Rejmund, *et al.*, Phys. Lett. B **697**, 454 (2011)
[7] K. Wei, J. H. Chen, and Y. L. Ye, Nucl. Phys. Rev. **42**(1), 1 (2025)
[8] J. Chen, J. L. Lou, Y. L. Ye *et al.*, Phys. Rev. C **93**, 034623 (2016)
[9] J. Chen, J. L. Lou, Y. L. Ye *et al.*, Phys. Rev. C **94**, 064620 (2016)
[10] J. Chen, J. L. Lou, Y. L. Ye *et al.*, Phys. Lett. B **781**, 412 (2018)
[11] J. Chen, J. L. Lou, Y. L. Ye *et al.*, Phys. Rev. C **98**, 014616 (2018)
[12] Y. Jiang, J. L. Lou, Y. L. Ye *et al.*, Chin. Phys. Lett. **35**(8), 082501 (2018)
[13] J. Chen, S. M. Wang, H. T. Fortune *et al.*, Phys. Rev. C **103**, L031302 (2021)
[14] W. Liu, J. L. Lou, Y. L. Ye *et al.*, Phys. Rev. C **104**, 064605 (2021)
[15] W. Liu, J. L. Lou, Y. L. Ye *et al.*, Phys. Rev. C **105**, 034613 (2022)
[16] B. L. Xia, J. L. Lou, Y. L. Ye *et al.*, Phys. Rev. C **108**, 064605 (2023)
[17] G. Li, J. L. Lou, Y. L. Ye *et al.*, Nucl. Instr. Meth. A **1013**, 165637 (2021)
[18] H. Y. Zhu, J. L. Lou, Y. L. Ye *et al.*, Nucl. Sci. Tech. **34**, 159 (2023)
[19] W. L. Pu, Y. L. Ye, J. L. Lou *et al.*, Nucl. Sci. Tech. **35**, 12 (2024)
[20] W. L. Zhan, Z. Y. Guo, Nucl. Phys. Rev. **16**(4), 218 (1999)(in Chinese)
[21] T. Shimoda, H. Miyatake, and S. Morinobu, Nucl. Inst. Meth. B **70**, 320 (1992)
[22] H. J. Ong, AIP Conf. Proc. **1588**, 146 (2014)
[23] C. J. Shao, R. C. Lu, X. H. Cai *et al.*, Nucl. Instr. Meth. A **317**, 617 (2013)
[24] L. J. Mao, H. Zhao, X.D. Yang *et al.*, Nucl. Instr. Meth. A **808**, 29 (2016)
[25] J. W. Xia, W. L. Zhan, B. W. Wei *et al.*, Nucl. Instr. Meth. A **488**, 11 (2002)
[26] J. T. Zhang, P. Ma, Y. Huang *et al.*, Phys. Rev. C **108**, 014614 (2023)
[27] K. Yue, J. T. Zhang, X. L. Tu *et al.*, Phys. Rev. C **100**, 054609 (2019)
[28] J. T. Zhang, K. Yue, H. X. Li *et al.*, Nucl. Instr. Meth. A **948**, 162848 (2019)
[29] Y. Huang, S.Y. Xia, Y. F. Li *et al.*, Phys. Lett. B **856**, 138902 (2024)
[30] J. T. Zhang *et al.*, Nucl. Instr. Meth. B **478**, 46 (2020)
[31] B. P. Kay, J. P. Schiffer, S. J. Freeman *et al.*, Phys. Rev. Lett **111**, 042502 (2013)
[32] J. Lee, M. B. Tsang , D. Bazin *et al.*, Phys. Rev. Lett **104**, 112701 (2010)
[33] E. Piasetzky, M. Sargsian, L. Frankfurt *et al.*, Phys. Rev. Lett **97**, 162504 (2006)
[34] http://nucleartheory.eps.surrey.ac.uk/NPG/index.htm.
[35] R. Varner, W. Thompson, T. McAbee *et al.*, Phys. Rep. **201**, 57 (1991)
[36] W. W. Daehnick, J. D. Childs, and Z. Vrcelj, Phys. Rev.C **21**, 2253 (1980)
[37] D. Y. Pang, P. Roussel-Chomaz, H. Savajols *et al.*, Phys. Rev. C **79**, 024615 (2009)
[38] J. Eichler and Th. Stöhlker, Phys. Rep. **439**, 1 (2007)